Iran J Sci Technol Trans Sci (2020) 44:549–555
https://doi.org/10.1007/s40995-020-00842-2

RESEARCH PAPER

Multiperiodic Spin Precession of the Optically Induced Spin Polarization in $Al_xGa_{1-x}As$/AlAs Single Quantum Well

S. Ullah[1,2] · G. M. Gusev[1] · A. K. Bakarov[3] · F. G. G. Hernandez[1]

Received: 9 October 2019 / Accepted: 21 February 2020 / Published online: 13 March 2020

Abstract
We employed the reflective probing of linearly polarized light to explore the dependence of electron spin dynamics, in a high mobility dense two-dimensional electron gas, on the external magnetic field, excitation power and sample temperature using the time-resolved Kerr rotation. Owing to the complex layered structure, the dynamics of spin polarization in the studied sample enclosed information about the spin signal corresponding to the different populations of electrons. Fit to the data revealed multiperiodic spin precession, with distinct g-factors that modulate the decay of the TRKR envelope. Additionally, the spin precession in our structure was seen to be thermally robust, persisting up to 250 K. The dynamics of optically induced spins, from different electron populations, was monitored as a function of different experimental parameters.

Keywords Spin polarization · Spin dephasing time · Quantum well · g-factor

1 Introduction

Optical spin pumping of carriers in semiconductor nanostructures is one of the key characteristics involved in numerous concepts for the realization and development of spin devices (Ullah et al. 2018; Meyer 1984; Ullah et al. 2016). On account of that, the preservation of spin information up to about room temperature is highly desirable and crucial from the viewpoint of its successful implementation into a practical platform (Ullah et al. 2018). More recently, the spin dynamics and related physics in semiconductors have evoked a great deal of interest, in part because of its possible applications in the information technology. And, also due to the fact that in semiconductors, different charge carriers such as electrons (Ullah et al. 2018; Larionov and Zhuravlev 2013), holes (Syperek et al. 2007; Yugova et al. 2012) and even their complexes like excitons and trions (Zhukov et al. 2007; Bar-Ad and Bar-Joseph 1992) can be spin-polarized and can be used to store and process information. Applications include the optical switching (Nishikawa et al. 1995), polarization control in the surface-emitting semiconductor laser (San Miguel et al. 1995), and the quantum memory devices and quantum computing (Wu et al. 2010; Žutić et al. 2004). Small relaxation time is required for the former cases, while the latter need a sufficiently long relaxation time to process the stored information.

The observation of extraordinary long spin dephasing time (T_2^*) in the bulk n-GaAs (Kikkawa and Awschalom 1998) has motivated the scientific community to investigate the spin dynamics in various GaAs-based systems like quantum wells (Hernandez et al. 2016; Ullah et al. 2017a, b, 2018), quantum dots (Feng et al. 2012, 2013), quantum wires (Csontos and Zülicke 2008; Fajardo et al. 2017; Kammermeier et al. 2018) and layered structures (Ullah et al. 2018; Berezovsky et al. 2006). However, to our knowledge, the isolation of spin contribution from the different population of electrons, in the symmetric QW structure, has not been reported so far. The reason behind spin contribution from different populations of electrons is that such multilayered AlGaAs/AlAs QW structure has

✉ S. Ullah
saeedullah.phy@gmail.com

[1] Instituto de Física, Universidade de São Paulo, Caixa Postal 66318, CEP 05315-970 São Paulo, SP, Brazil

[2] Institute of Physics and Electronics, Gomal University, Dera Ismail Khan 29220, KP, Pakistan

[3] Institute of Semiconductor Physics and Novosibirsk State University, Novosibirsk 630090, Russia

several GaAs layers having the optical transition at nearly same photon energy and thus impedes the identification of layers when tuned by the excitation energy using the short laser pulses. As a result, we detect the spin signal containing contribution from the electron population in different layers.

In the studied structure, we found that the electron spins corresponding to two different layers contribute to the total Kerr signal, i.e., the two-dimensional electron gas (2DEG) layer and the GaAs substrate. We utilized the electron g-factor as a tool to identify the signal belonging to each population. The same approach has been used in Ref. Syperek et al. (2007) to distinguish the photo-excited electrons and holes. Based on our results, one can define the regime and conditions where the individual spin population can be studied without being interrupted by the above-said effects. Our results indicate that the spin signal from an individual layer can be studied independently when the excitation density gives rise to the photo-created density smaller than that of the doping density of 2DEG. The regime where the photo-generated carrier density becomes equal or exceeds the 2DEG density one can evidence the contribution from other layers.

The rest of paper is organized as follows: The next section describes the materials and experimental details followed by the experimental results regarding the spin signal corresponding to a different population of electrons and its dependence on various experimental parameters. Concluding remarks are given in the last section.

2 Materials and Experiment

The spin dynamics was investigated here with experimental results on a 14-nm-wide AlGaAs/AlAs single quantum well. The schematic layered structure of the sample is shown in Fig. 1. The sample is remotely delta-doped containing three doping layers inserted into the barriers of the quantum well. The doping layers in the vicinity of the QW render carriers for the 2DEG, while the doping layer nearby the surface of the structure was carried out to saturate the dangling bonds. The electrons from the doping layers were assembled into the QW, creating a dense 2DEG with a total electron density of $n_s = 4.79 \times 10^{11}\,\mathrm{cm}^{-2}$ and the mobility $\mu = 35.8 \times 10^3\,\mathrm{cm}^2/\mathrm{Vs}$. The quantum well was grown by molecular beam epitaxy (MBE) with x = 10% Al content inside the well. The purpose of adding Al contents inside the well is to tune the g-factor of the QW confined electrons. A detailed study regarding the tailoring of electron g-factor in $Al_xGa_{1-x}As$/AlAs single and double quantum wells with

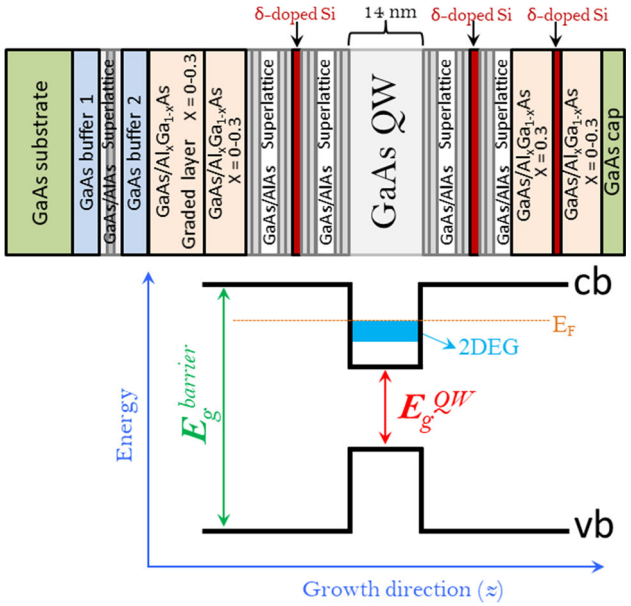

Fig. 1 Schematic layered structure of AlGaAs/AlAs single QW grown by molecular beam epitaxy along the z-axis

different aluminum contents ($8.2\% < x < 16\%$) will be published elsewhere.

We employed the pump-probe Kerr rotation technique, a well-established tool (Baumberg et al. 1994), to investigate the electron spin dynamics. The spin polarization was generated by circularly polarized pump pulses emitted from a mode-locked Ti: Sapphire laser with pulse duration of 100 fs, operating at a repetition frequency of 76 MHz ($t_{\mathrm{rep}} = 13.2$ ns) as shown schematically in Fig. 2a. The pump pulses were focused on the sample surface to a spot size of $\sim 20\,\mu$m. The induced spin coherence was measured by relatively weak linearly polarized probe pulses of the same photon energy as the pump pulses (degenerate pump-probe system). A computer-controlled mechanical delay line was used to monitor the time delay between the probe and pump pulses. The laser wavelength was tuned for the maximum Kerr signal with long coherence time. The pump beam was modulated by a photo-elastic modulator (PEM) operated at 50 kHz for lock-in detection. The Kerr rotation (KR) angle of the initially linearly polarized probe pulses upon the reflection from the sample surface was measured by a balanced bridge.

3 Results and Discussion

3.1 Dependence of Spin Dynamics on Excitation Energy

For the selection of the right excitation energy, the TRKR dependence on the laser wavelength was measured. A

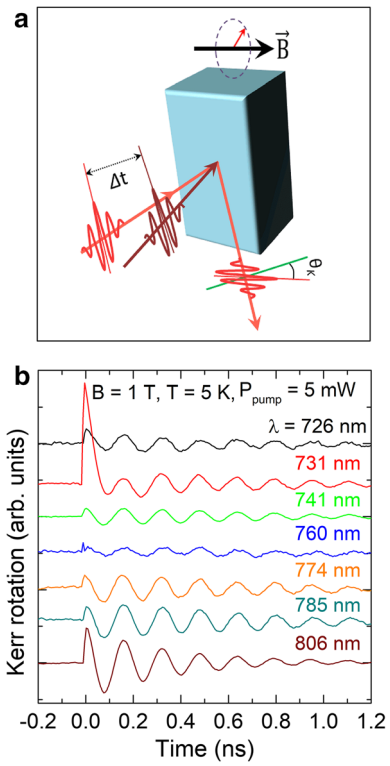

Fig. 2 **a** Schematic of the time-resolved Kerr rotation. **b** KR versus time delay between pump and probe for different excitation wavelengths. The powers were set to 5 and 1.3 mW for the pump and probe, respectively. $B = 1$ T and $T = 5$ K

series of TRKR traces were recorded for different excitation energies ranging from $\lambda = 726$ nm to 806 nm, with an excitation power of 5 mW under the applied magnetic field of $B = 1$ T and sample temperature $T = 5$ K (Fig. 2b). We found the TRKR trace with the maximum signal at $\lambda = 731$ nm. Additionally, the signal showed an unusual behavior with two contributions resulting from different electron population, each oscillating with its frequency and decay time. The short-living component contributes to the signal at very short pump-probe delay and oscillates in the initial few of tens picoseconds.

To have an idea of the spin dephasing time and the oscillation frequency of each component, a TRKR scan, with a pump power of 20 mW while keeping the magnetic field, wavelength and temperature the same as of Fig. 2b, was recorded as shown in Fig. 3. The total spin signal is well described by a superposition of two exponentially decaying cosine functions (Ullah et al. 2016, 2018a, b).

$$\Theta_K = \sum_{i=1}^{2} A_i \exp\left(\frac{-\Delta t}{T_{2,i}^*}\right) \cos\left(\frac{|g_i|\mu_B B}{\hbar}\Delta t + \varphi_i\right) + y_0 \quad (1)$$

where A_i is the initial amplitude, μ_B is the Bohr magneton, B is the external magnetic field, $\hbar$ is the reduced Planck's constant, $|g_i|$ is the electron factor, φ_i is the initial phase, y_0

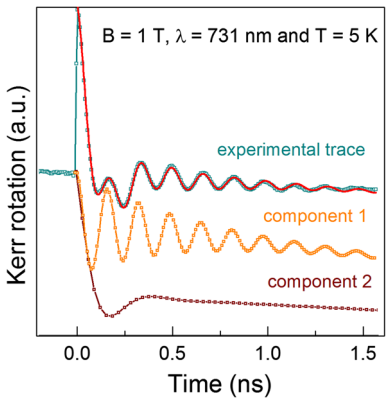

Fig. 3 Decomposition of TRKR signal recorded at $B = 1$ T, $\lambda = 731$ nm and $T = 5$ K. The top curve is the measured signal and the bottom traces are the components obtained from decomposition. The red curve plotted on the top of experimental trace corresponds to the exponentially damped cosine function displayed in Eq. 1

is the offset and $T_{2,i}^*$ is the ensemble dephasing time. The overall dynamics of spin polarization, plotted by the cyan color, represents the measured transient of Kerr rotation signal where the fitted curve shown by red color is plotted on the top of the experimental trace.

The extracted components from the decomposition of experimental data are shown by orange and wine colors. The fit extracts the spin relaxation times of 0.51 ± 0.01 ns and 0.116 ± 0.001 ns for components 1 and 2, respectively. Additionally, the data yield two frequencies 38.35 ± 0.04 GHz and 13.68 ± 0.17 GHz corresponding to the effective Landé factors (absolute values) of 0.434 ± 0.001 and 0.15 ± 0.01 for components 1 and 2, respectively.

3.2 Dependence of Spin Dynamics on External Magnetic Field

To give a deeper insight into the signals obtained in the TRKR trace shown in Fig. 3 and identify the nature of oscillation, the time evolution of KR signal was recorded as a function of external magnetic field for a low and high pump power. Figure 4a shows a set of TRKR traces measured for different magnetic fields in the range from 1 to 5 T at a pump power of 1 mW (corresponding to the pump density of 318.5 W/cm^2) while keeping the experimental conditions ($T = 5$ K and $\lambda = 731$ nm) the same as were in the previous section. The tuned pump density yields the photo-created carrier density of $1.63 \times 10^{10} cm^{-2}$ which is lower than the 2DEG density by almost an order of magnitude, and thus, one can evidence the spin signal containing information from an individual population of electrons. The curves were fitted to a single exponentially decaying cosine function (Ullah et al. 2016). The fitted values of ensemble dephasing time and Larmor precession frequency were plotted as a function of magnetic field

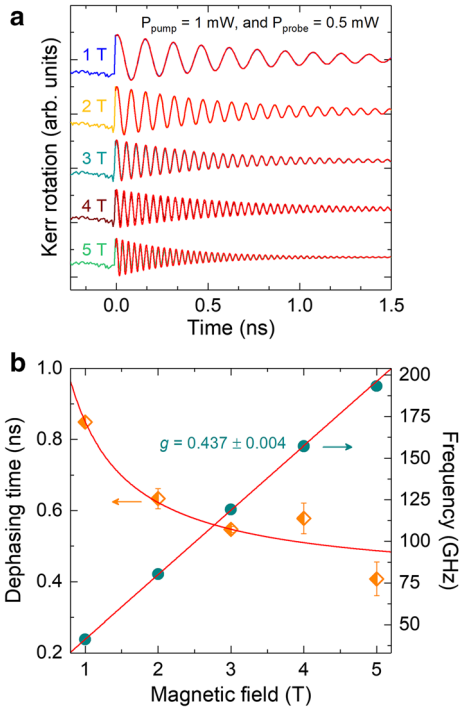

Fig. 4 **a** Time-resolved Kerr rotation measured for the various magnetic fields in the range from 1 to 5 T (pump/probe power = 1 mW/0.5 mW and $T = 5$ K). **b** Spin dephasing time (half-filled diamond) and Larmor frequency (solid circles) versus applied magnetic field. The fitted curve on T_2^* is $1/B$-like dependence

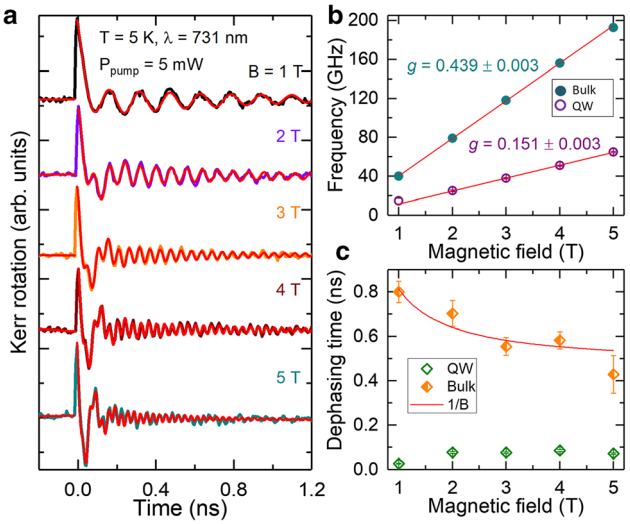

Fig. 5 **a** KR transients recorded at different magnetic fields. The traces are shifted vertically for clarity of presentation. The red lines plotted on the top of experimental data are fitted to Eq. 1. Magnetic field dependence of **b** Larmor precession frequency and **c** spin dephasing time. The solid red curve in (**c**) is the $1/B$-like fit which yields $\Delta g = 0.003$. $T = 5$ K, $P_{\text{pump}} = 5$ mW and $P_{\text{probe}} = 1.3$ mW

(Fig. 4b). The spin dephasing time yields a maximum value of 0.85 ns (at $B = 1$ T), which further decrease down to 0.41 ns (at $B = 5$ T) possibly due to the Dyakonov–Perel mechanism (D'yakonov 1971) as well as the ensemble spread (Δg) of g-factor (Zhukov et al. 2007; Greilich et al. 2006). The data follow $1/B$-like dependence, where the size of the spread $\Delta g = 0.004$ was deduced by fitting the data to $T_2^* = \sqrt{2}\hbar/\Delta g \mu_B B$ (Ullah et al. 2018; Bratschitsch et al. 2006), which is 0.91% of the observed g-value. One can clearly see that the spin beat frequency speed up with the growing magnetic field and follows a linear increase, which is distinctive for the electrons (Ullah et al. 2016, 2018a, b); however, irregularities can happen for the holes due to the band mixing as observed in InGaAs/GaAs QWs (Traynor et al. 1995). The g-factor evaluated from the linear interpolation recommends that only the bulk electrons are contributed in the signal.

The TRKR traces measured at $P_{\text{pump}} = 5$ mW (1592.5 W/cm^2), for various magnetic fields while keeping the other parameters unchanged, are displayed in Fig 5a. The used pump density induces a photo-generated carrier density ($\sim 0.1 \times 10^{11}$ cm^{-2}) of the order of the 2DEG density, and thus, two oscillatory signals with distinct frequencies were observed in the entire magnetic field range. Furthermore, at $B = 1$ T the short-living spin component oscillates with a very small frequency of 14 GHz. To extract the spin dephasing time and electron g-factor, the experimental curves are fitted to Eq. 1.

The resulted magnetic field dependence of Larmor precession frequency and spin dephasing time for both components is displayed in Fig. 5b, c. The electron g-factors (absolute values) evaluated from the linear dependence of Larmor precession frequencies on the magnetic field are 0.439 ± 0.003 GHz and 0.151 ± 0.003 GHz. The observed g-factors help us to understand the physics underlying the Kerr signal from two different populations. The g-factors of component 1 are in good agreement with the g-factor of the bulk ($|g| = 0.44$) (Ivchenko and Kiselev 1998), which indicates that the signal of component 1 corresponds to the electron population in the bulk, while the g-factor of component 2 is attributed to the signal from electron population in the quantum well. The spin dephasing time of the signal from the bulk shows an obvious decrease with increasing magnetic field, and thus, we recovered the data presented in Fig 4, while for the signal from QW we observed a slight increase in T_2^*.

3.3 Dependence of Spin Dynamics on Sample Temperature

To explore whether the contributions to the spin signal (observed in the previous section) are robust against temperature, a set of TRKR scan was recorded as a function of sample temperature over the range of 5–250 K as shown in Fig. 6. In order to highlight the trends at positive time

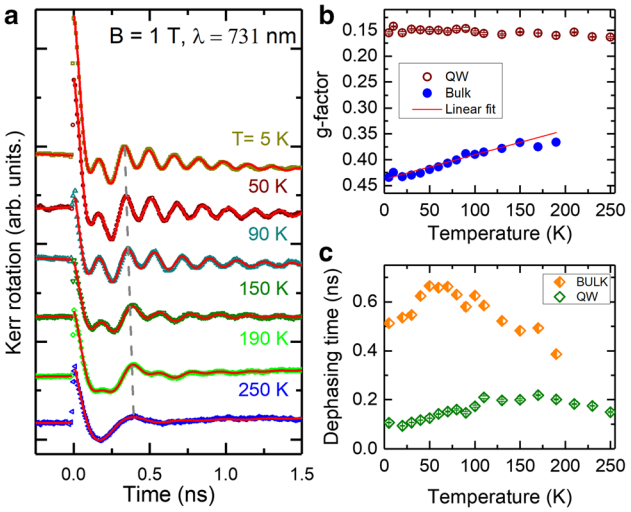

Fig. 6 Temperature dependence of spin dynamics: **a** TRKR signals recorded as a function of sample temperature in the range from 5 K up to 250 K. The symbols are experimental data, and the solid lines are fitted to Eq. 1. The extracted **b** g-factor and **c** dephasing time as a function of temperature. $B = 1$ T, $P_{\text{pump}} = 20.2$ mW and $P_{\text{probe}} = 1.3$ mW

delay, the TRKR traces were normalized to the time origin ($\Delta t = 0$ ns). From the experimental traces, the following significant features are directly evident. First, in the temperature range, 5 K $< T <$ 190 K, both signals (bulk and QWs) are contributing to the total spin polarization. Second, the spin precession frequency changes with the rise of temperature as shown by the dashed line. Third, compared to the bulk, the signal from the quantum well is robust against temperature and is traced up to 250 K, while the bulk signal is getting weaker with the rising temperature and disappears above 190 K.

Fit to the data shown in Fig. 6a yields the electron g-factors and spin dephasing times, which are displayed in Fig. 6b, c as a function of temperature. One can clearly see from this dependence that there is almost no influence of the sample temperature on the g-factor of QW. However, the bulk g-factor increases with temperature and follows a linear dependence with, $g(\text{T}) = -0.438 + 4.76 \times 10^{-4}\,\text{T}$, which is in complete agreement with previously published data on bulk GaAs (Oestreich et al. 1996). The evaluated spin dephasing times, as depicted in Fig. 6c, show pronounced temperature dependence. T_2^* for both the QW and bulk signals first increases with the temperature reaching to its maximum value and then starts to decrease with a further rise of temperature; however, the reduction is much strong in the bulk and the signal completely disappears after 190 K. The increase in dephasing time with rising temperature designates the suppression of the Dyakonov–Perel mechanism mainly due to the fast momentum scattering. Above a certain temperature, the thermal spread in the spin-oriented electrons kinetic energy lead to the spread in g-factor value which further results in the precessional dephasing (Ullah et al. 2018; Bratschitsch et al. 2006).

3.4 Dependence of Spin Dynamics on Optical Pump Power

The robustness of spin polarization against temperature was studied in the previous section where the signal from the QW was found to persist up to 250 K; however, the signal from bulk did not last long and was traced only up to 190 K. After a certain limit of temperature, both the signals showed reduction with temperature possibly due to the heating effect. As an additional inquiry to confirm the reduction in spin dephasing time due to heating effect, the TRKR traces were measured as a function of excitation power in a wide range from 1 mW up to 73 mW as shown in Fig. 7a. For the clarity of presentation, the curves recorded at low pump power are upscaled by multiplying with certain numbers as mentioned inside the panel. With increasing pump power, the bulk signal is getting weaker and disappears at 73 mW.

The spin dephasing time, extracted from (a), for both the bulk and quantum well signals, is shown in Fig. 7b. T_2^* received from the QW signal increases slightly from 36 ps at 1 mW up to 129 ps at 73 mW. However, plotting together with T_2^* received from the bulk signal may be

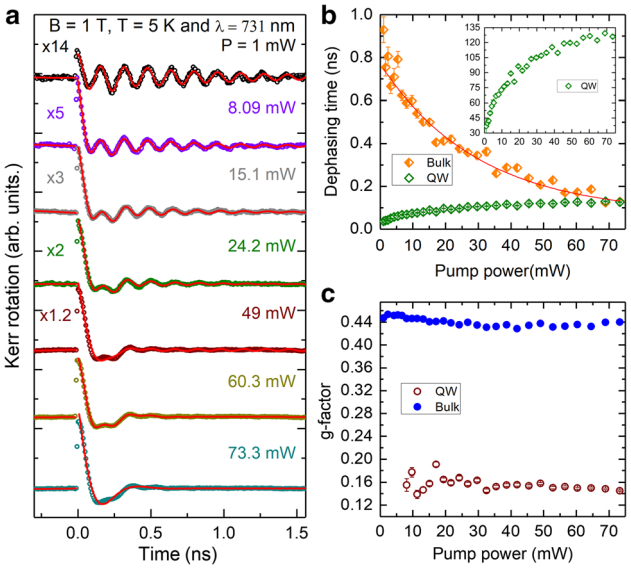

Fig. 7 Pump power influence on spin dynamics: **a** TRKR signals as a function of excitation power in the range from 1 mW up to 73 mW. To enhance the clarity of presentation, multiplicative factors (labeled inside the panel) are used for the low pump power. The evaluated **b** spin dephasing times, where the inset highlights that T_2^* received from the quantum well signal increases with increasing the pump power, and **c** the electron g-factors as a function of excitation power. $T = 5$ K, $B = 1$ T and $\lambda = 731$ nm

hiding this trend. See, for example, the dephasing time versus pump power (inset Fig. 7b) where the trend is clearly visible. Furthermore, T_2^* retrieved from the bulk signal decreases exponentially as shown by the solid red curve. For a single QW structure, a similar decrease was assigned to the heating effect induced by optical excitation (Zhukov et al. 2007). The observed behavior of T_2^* with increasing pump power is in good agreement with the previously reported data on a wide GaAs quantum well (Ullah et al. 2016). The resulting pump power dependence of g-factor is shown in Fig 7c. From this dependence, it is clear that there is no influence of excitation pump power on the g-factor (absolute value) evaluated from the QW signal. However, the g-factor obtained from bulk signal decreases up to 35 mW and then saturates with the further rise of pump power.

4 Conclusions

In conclusion, we have carried out a detailed study of spin dynamics in a high mobility dense two-dimensional electron gas confined in AlGaAs/AlAs single quantum well by employing a reflective pump-probe technique: TRKR. We used the electron g-factor as a tool to analyze the physics underlying the Kerr response from two different population of electrons. Our results allowed us to define the conditions and regime where the spin polarization from different electron populations can be induced. Additionally, we studied that how the spin dephasing time and electron g-factor from two different electron populations depend on the experimental parameters like excitation power, sample temperature and external magnetic field. Furthermore, we noticed that the spin polarization signal from the 2DEG is robust against temperature and can be obviously traced up to T = 250 K. In contrast, the signal from the bulk displayed a fast decoherence and completely disappeared above 190 K.

Acknowledgements F.G.G.H. acknowledges financial support from Grant Nos. 2009/15007-5, 2013/03450-7, 2014/25981-7 and 2015/16191-5 of the São Paulo Research Foundation (FAPESP). S.U acknowledges TWAS/CNPq for financial support.

References

Bar-Ad S, Bar-Joseph I (1992) Exciton spin dynamics in GaAs heterostructures. Phys Rev Lett 68:349

Baumberg JJ, Awschalom DD, Samarth N, Luo H, Furdyna JK (1994) Spin beats and dynamical magnetization in quantum structures. Phys Rev Lett 72:717

Berezovsky J, Gywat O, Meier F, Battaglia D, Peng X, Awschalom DD (2006) Initialization and read-out of spins in coupled core–shell quantum dots. Nat Phys 2:831–834

Bratschitsch R, Chen Z, Cundiff ST, Zhukov EA, Yakovlev DR, Bayer M, Karczewski G, Wojtowicz T, Kossut J (2006) Electron spin coherence in n-doped CdTe/CdMgTe quantum wells. Appl Phys Lett 89:221113

Csontos D, Zülicke U (2008) Tailoring hole spin splitting and polarization in nanowires. Appl Phys Lett 92:023108

D'yakonov MI (1971) Spin orientation of electrons associated with the interband absorption of light in semiconductors. Sov Phys JETP 33:1053–1059

Fajardo EA, Zuelicke U, Winkler R (2017) Universal spin dynamics in quantum wires. Phys Rev B 96:155304

Feng DH, Li X, Jia TQ, Pan XQ, Sun ZR, Xu ZZ (2012) Long-lived, room-temperature electron spin coherence in colloidal CdS quantum dots. Appl Phys Lett 100:122406

Feng DH, Shan LF, Jia TQ, Pan XQ, Tong HF, Deng L, Sun ZR, Xu ZZ (2013) Optical manipulation of electron spin coherence in colloidal CdS quantum dots. Appl Phys Lett 102:062408

Greilich A, Oulton R, Zhukov EA, Yugova IA, Yakovlev DR, Bayer M, Shabaev A, Efros AL, Merkulov IA, Stavarache V, Reuter D (2006) Optical control of spin coherence in singly charged (In, Ga)As/GaAs quantum dots. Phys Rev Lett 96:227401

Hernandez FGG, Ullah S, Ferreira GJ, Kawahala NM, Gusev GM, Bakarov AK (2016) Macroscopic transverse drift of long current-induced spin coherence in two-dimensional electron gases. Phys Rev B 94:045305

Ivchenko EL, Kiselev AA (1998) Electron g factor in quantum wires and quantum dots. J Exp Theor Phys Lett 67:43–47

Kammermeier M, Wenk P, Dirnberger F, Bougeard D, Schliemann J (2018) Spin relaxation in wurtzite nanowires. Phys Rev B 98:035407

Kikkawa JM, Awschalom DD (1998) Resonant spin amplification in n-type GaAs. Phys Rev Lett 80:4313

Larionov AV, Zhuravlev AS (2013) Coherent spin dynamics of different density high mobility two-dimensional electron gas in a GaAs quantum well. JETP Lett 97:137–140

Meyer M, Zakharchenya BP (1984) Optical orientation. North-Holland, Amsterdam

Nishikawa Y, Tackeuchi A, Nakamura S, Muto S, Yokoyama N (1995) All-optical picosecond switching of a quantum well etalon using spin-polarization relaxation. Appl Phys Lett 66:839–841

Oestreich M, Hallstein S, Heberle AP, Eberl K, Bauser E, Rühle WW (1996) Temperature and density dependence of the electron Landé g factor in semiconductors. Phys Rev B 53:7911

San Miguel M, Feng Q, Moloney JV (1995) Light-polarization dynamics in surface-emitting semiconductor lasers. Phys Rev A 52:1728

Syperek M, Yakovlev DR, Greilich A, Misiewicz J, Bayer M, Reuter D, Wieck AD (2007) Spin coherence of holes in GaAs/(Al, Ga)As quantum wells. Phys Rev Lett 99:187401

Traynor NJ, Harley RT, Warburton RJ (1995) Zeeman splitting and g factor of heavy-hole excitons in In_x $Ga_{1-x}As$/GaAs quantum wells. Phys Rev B 51:7361

Ullah S, Gusev GM, Bakarov AK, Hernandez FGG (2016) Long-lived nanosecond spin coherence in high mobility 2DEGs confined in double and triple quantum wells. J Appl Phys 119:215701

Ullah S, Gusev GM, Bakarov AK, Hernandez FGG (2017a) Large anisotropic spin relaxation time of exciton bound to donor states in triple quantum wells. J Appl Phys 121:205703

Ullah S, Ferreira GJ, Gusev GM, Bakarov AK, Hernandez FGG (2017b) Macroscopic transport of a current-induced spin polarization. J Phys Confer Ser 864:012060

Ullah S, Gusev GM, Bakarov AK, Hernandez FGG (2018a) Tailoring multilayer quantum wells for spin devices. Pramana 91:34. https://doi.org/10.1007/s12043-018-1611-4

Ullah S, Moraes FCD, Gusev GM, Bakarov AK, Hernandez FGG (2018b) Robustness of spin polarization against temperature in multilayer structure: triple quantum well. J Appl Phys 123:214306

Ullah S, Gusev GM, Bakarov AK, and Hernandez FGG (2018c) Optically-detected long-lived spin coherence in multilayer systems: double and triple quantum wells. In: National conference on mathematical sciences in engineering applications (NCMSEA - 18) proceeding 275. arXiv:1806.03092

Wu MW, Jiang JH, Weng MQ (2010) Spin dynamics in semiconductors. Phys Rep 493:61–236

Yugova IA, Glazov MM, Yakovlev DR, Sokolova AA, Bayer M (2012) Coherent spin dynamics of electrons and holes in semiconductor quantum wells and quantum dots under periodical optical excitation: resonant spin amplification versus spin mode locking. Phys Rev B 85:125304

Zhukov EA, Yakovlev DR, Bayer M, Glazov MM, Ivchenko EL, Karczewski G, Wojtowicz T, Kossut J (2007) Spin coherence of a two-dimensional electron gas induced by resonant excitation of trions and excitons in CdTe/(Cd, Mg)Te quantum wells. Phys Rev B 76:205310

Žutić I, Fabian J, Sarma SD (2004) Spintronics: fundamentals and applications. Rev Modern Phys 76:323